



Toroidal mode number estimation of the edge-localized modes using the KSTAR 3-D electron cyclotron emission imaging system

J. Lee, G. S. Yun, J. E. Lee, M. Kim, M. J. Choi, W. Lee, H. K. Park, C. W. Domier, N. C. Luhmann jr., S. A. Sabbagh, Y. S. Park, S. G. Lee, and J. G. Bak

Citation: *Review of Scientific Instruments* **85**, 063505 (2014); doi: 10.1063/1.4883180

View online: <http://dx.doi.org/10.1063/1.4883180>

View Table of Contents: <http://scitation.aip.org/content/aip/journal/rsi/85/6?ver=pdfcov>

Published by the [AIP Publishing](#)

Articles you may be interested in

[Nonlinear excitation of low-n harmonics in reduced magnetohydrodynamic simulations of edge-localized modes](#)
Phys. Plasmas **20**, 082506 (2013); 10.1063/1.4817953

[Two-dimensional imaging of edge-localized modes in KSTAR plasmas unperturbed and perturbed by n=1 external magnetic fields](#)

Phys. Plasmas **19**, 056114 (2012); 10.1063/1.3694842

[Driving toroidally asymmetric current through the tokamak scrape-off layer. I. Potential for edge localized mode suppression](#)

Phys. Plasmas **16**, 052510 (2009); 10.1063/1.3134580

[Upgrades to the TEXTOR electron cyclotron emission imaging diagnostic](#)

Rev. Sci. Instrum. **77**, 10E924 (2006); 10.1063/1.2352727

[Measurements of edge-localized-mode induced electron cyclotron emission bursts in DIII-D](#)

Phys. Plasmas **8**, 1594 (2001); 10.1063/1.1362527



AIP | Journal of
Applied Physics

Journal of Applied Physics is pleased to
announce **André Anders** as its new Editor-in-Chief

Toroidal mode number estimation of the edge-localized modes using the KSTAR 3-D electron cyclotron emission imaging system

J. Lee,¹ G. S. Yun,^{1,a)} J. E. Lee,¹ M. Kim,¹ M. J. Choi,¹ W. Lee,¹ H. K. Park,² C. W. Domier,³ N. C. Luhmann, jr.,³ S. A. Sabbagh,⁴ Y. S. Park,⁴ S. G. Lee,⁵ and J. G. Bak⁵

¹*Pohang University of Science and Technology, Pohang 790-784, South Korea*

²*Ulsan National Institute of Science and Technology, Ulsan 689-798, South Korea*

³*University of California at Davis, Davis, California 95616, USA*

⁴*Columbia University, New York, New York 10027, USA*

⁵*National Fusion Research Institute, Daejeon 305-333, South Korea*

(Received 17 March 2014; accepted 1 June 2014; published online 18 June 2014)

A new and more accurate technique is presented for determining the toroidal mode number n of edge-localized modes (ELMs) using two independent electron cyclotron emission imaging (ECEI) systems in the Korea Superconducting Tokamak Advanced Research (KSTAR) device. The technique involves the measurement of the poloidal spacing between adjacent ELM filaments, and of the pitch angle α_* of filaments at the plasma outboard midplane. Equilibrium reconstruction verifies that α_* is nearly constant and thus well-defined at the midplane edge. Estimates of n obtained using two ECEI systems agree well with n measured by the conventional technique employing an array of Mirnov coils.

© 2014 AIP Publishing LLC. [<http://dx.doi.org/10.1063/1.4883180>]

I. INTRODUCTION

Edge-localized modes (ELMs)^{1,2} are repetitive and explosive instabilities induced by pressure gradients, current density, or both at the pedestal region of magnetic confinement plasmas. ELM crashes can induce substantial loss of confinement of edge particles and heat, and can damage components that face the plasma; this damage is a serious impediment to steady-state operation of fusion devices.³ Linear stability analysis based on peeling-ballooning (PB) mode theory has successfully explained the emergence of typical type-I ELMs.⁴ PB mode theory predicts that the PB mode will evolve into filamentary structures along the helical magnetic field lines,⁵ and this process has been observed in several tokamaks.^{6–8} Although PB theory has explained the onset conditions and mode structure for ELMs, experimental observations suggest that ELM dynamics are far more complicated than the theory depicts. Detailed observation of ELM dynamics and accurate measurement of the mode structure will enhance the understanding for ELMs physics.

The entire ELM evolution process was recently studied in detail⁸ using a 2D visualization tool called electron cyclotron emission imaging (ECEI) system⁹ in the Korea Superconducting Tokamak Advanced Research (KSTAR) device. Results revealed the detailed phenomenology of the ELM structure and dynamics such as radial and poloidal extent, poloidal flow, poloidal elongation of filaments before the crash, and the localized crash induced by a pressure finger-like structure. However, other crucial quantities for the study of linear and nonlinear ELM physics, such as toroidal mode number n , pitch angle α , and toroidal asymmetry of the ELM structure, were difficult to measure accurately because of the 3D nature

of the ELM structure. In particular, an accurate measurement of n was often very difficult or impossible to achieve using the conventional analysis of Mirnov coil array signals when the perturbation amplitude was weak or when n was larger than the Nyquist limit.

This paper presents a new method to determine n using two ECEI systems. The fundamentals of the ECEI system are explained in Sec. II. The method for estimating n of the ELMs is described and its validity is assessed by equilibrium fitting (EFIT) code calculation in Sec. III. Experimentally measured n values from two ECEI systems and Mirnov coils are compared in Sec. IV. The work is summarized in Sec. V.

II. ECEI SYSTEM

ECEI is an advanced diagnostic tool to visualize magnetohydrodynamic (MHD) instabilities such as sawtooth,¹⁰ ELMs,¹¹ tearing modes,¹² and Alfvén eigenmodes¹³ by measuring the electron temperature fluctuation $\delta T_e = T_e - \langle T_e \rangle$ in 2D, where $\langle T_e \rangle$ is a time average.

The KSTAR ECEI system has dual independent heterodyne detector arrays, which provide simultaneous measurements of the high-field side and low-field side of the plasma. Due to a flexible large aperture optics system, two ECEI view positions can be focused anywhere in the poloidal cross-section with vertical coverage from ~ 30 to 90 cm. Each detector array has 24 (vertical) \times 8 (radial) = 192 channels for electron temperature fluctuation measurement with a spatial resolution $\sim 1 - 2$ cm and temporal resolution $\sim 1 - 2 \mu\text{s}$. In addition, another ECEI system has been installed in KSTAR, toroidally separated from the 1st ECEI by 1/16th of the torus, to extend the diagnostic capability in 3D. Using the two ECEI systems, ELM filaments were visualized in quasi 3D for the first time during the 2012 KSTAR campaign.

^{a)} Author to whom correspondence should be addressed. Electronic mail: gunsu@postech.ac.kr

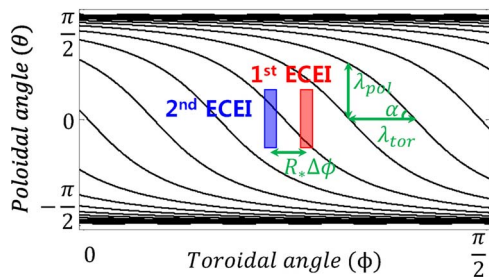


FIG. 1. Conceptual diagram of the pitch angle and toroidal mode number estimation using two independent ECEI systems. Black lines: magnetic field lines; blue and red boxes: 1st and 2nd ECEI view, respectively. ELM filaments are assumed to be aligned along the magnetic field lines.

III. TOROIDAL MODE NUMBER ESTIMATION USING 3D ECEI

Mirnov coils are an array of magnetic pickup probes installed along the tokamak vacuum vessel wall either toroidally or poloidally. They are relatively simple to construct and are commonly used to measure the geometrical structure of a MHD instability mode, in particular n , which is a critical parameter for MHD stability analysis in toroidal plasmas. However, Mirnov coils, albeit an essential tokamak diagnostic, have a number of limitations. Because each coil can measure only the time-varying magnetic fields at a fixed location, the coil sensitivity to a MHD mode strongly depends on the rotation frequency of the MHD mode in the laboratory frame. For this reason, it would be difficult to detect a MHD mode with very low rotation frequency using Mirnov coils. In addition, the coil sensitivity degrades for higher n MHD instabilities as $\tilde{B} \propto 1/\rho^n$,^{14,15} where \tilde{B} is the magnetic perturbation amplitude, and ρ is the distance from the mode structure to the detector array. Mirnov coils also have a Nyquist limit due to the finite number of coils. For example, KSTAR is equipped with one toroidal array of 20 Mirnov coils and thus the detectable range of n is limited up to 10.

A convenient definition of the toroidal mode number is given below (see Fig. 1)

$$n = \frac{2\pi R_*}{\lambda_{tor}}, \quad (1)$$

where R_* [cm] is the major radius of the instability mode at the outboard midplane, and λ_{tor} [cm] is the toroidal spacing between peaks (or valleys) of the instability mode, i.e., the toroidal wavelength.

In poloidal and toroidal angle coordinate space, filamentary instability modes like ELMs at the outboard midplane have the following relationship among λ_{tor} , poloidal mode spacing λ_{pol} , and pitch angle of the filaments at the outboard midplane α_* (see Fig. 1):

$$\lambda_{tor} = \lambda_{pol} / \tan \alpha_*. \quad (2)$$

Combining Eqs. (1) and (2) yields

$$n = \frac{2\pi R_*}{\lambda_{pol}} \cdot \tan \alpha_*. \quad (3)$$

For ELMs, R_* , λ_{pol} , and $\tan \alpha_*$ can be accurately measured using two ECEI systems alone.

Equation (3) is only valid if α_* is nearly constant around the midplane; if α_* varies substantially around the midplane, it is hard to determine α_* , and thereby n can be easily misinterpreted. Along the field line in the poloidal direction, α_* reconstructed by EFIT^{16,17} (Fig. 2(a)) varies by less than 4% within the ECEI view (typical vertical span ~ 40 cm).

IV. COMPARISON ANALYSIS BETWEEN THE ECEI ESTIMATION AND MIRNOV COILS MEASUREMENT

In typical KSTAR discharges, the direction of toroidal magnetic field B_{tor} and plasma current I_p are clockwise as viewed from Fig. 3(a); therefore, the ELM filament captured by the 2nd ECEI system is the same as the lower ELM filament in the 1st ECEI system (Fig. 3(b)). λ_{pol} can be measured directly from the ECEI snapshot. Because the field line shape is already known and the two ECEI systems are toroidally separated by 1/16th of the torus (or by an angle $\Delta\phi = \pi/8$ rad), the pitch angle can be determined by measuring the

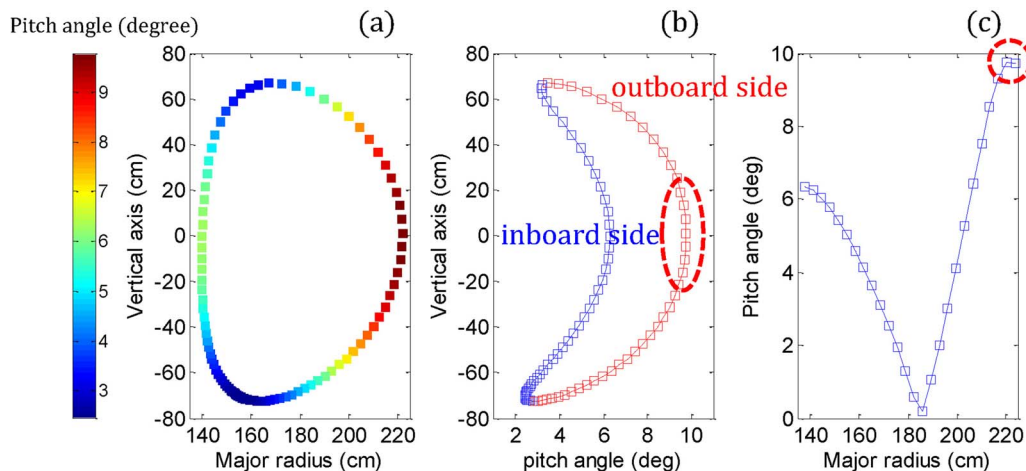


FIG. 2. (a) Variation of pitch angle (presented by color codes) along the poloidal angle on the $q = 95\%$ flux surface, calculated by EFIT (for shot #7328 at time ~ 4.4 s). (b) Pitch angle variation along the vertical axis; red line: outboard side of the plasma; blue line: inboard side of the plasma. (c) Radial variation of pitch angle; this shows that the pitch angle is nearly constant at the midplane and edge.

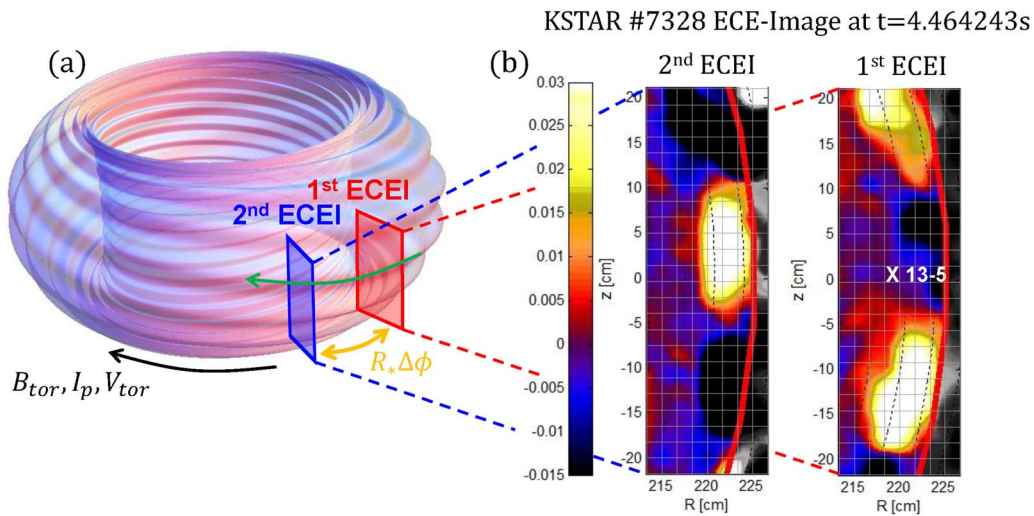


FIG. 3. (a) Illustration of helical perturbation in the edge of the KSTAR plasma. The direction of toroidal magnetic field, plasma current, and toroidal flow velocity are all clockwise. (b) ECEI snapshot of ELM filaments for $n = 7$ case. The color map represents the relative amplitude of ECE intensity fluctuations ($\delta T_e / \langle T_e \rangle$). The red line shows the separatrix position determined by EFIT.

change in vertical distance of the same flux tube in the two ECEI views.

A correlation technique is used to increase the accuracy of the mode spacing measurement. In order to obtain the spatial correlation, the normalized temporal correlation coefficients were calculated along the poloidal direction in the 1st ECEI system using channel #13-5 of the 2nd ECEI system as the reference. The spatial correlation can be derived from the temporal correlation coefficients of individual channels with zero time lag. Assuming that the ELM filaments are identical and homogenous along the magnetic field lines, the spatial correlation between ECEI signals in the vertical (poloidal) direction is expected to form a sinusoidal variation as in Fig. 4. Fig. 4 shows that the maximum correlation coefficients occur at the vertical channels #5 and #19. Noting that the vertical channel #19 does not match with the field line pitch (cf. Figs. 1 and 2(c)), it can be concluded that the vertical channel #5 is to be on the same filament (or flux tube) as the reference channel. Similarly, the accuracy of the measurement of

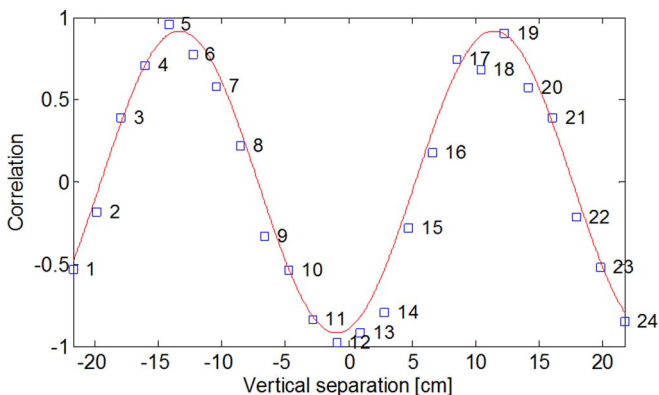


FIG. 4. Normalized Pearson product-moment correlation coefficients ($\frac{1}{N} R_{xy}$, where N is a length of signal) at the zero time lag between the 13-5 channel in the 1st ECEI system and the channels in the 2nd ECEI along the same poloidal flux surface. The pitch angle can be estimated by measuring the vertical distance of the channel with maximum correlation from the reference channel.

the poloidal spacing between the ELM filaments is increased using the same correlation method within one ECE image.

For the example case of Fig. 3(b), λ_{pol} is ~ 34.1 cm, the vertical spacing of the same flux tube between the two ECEI views Δy is ~ 15.1 cm, and the toroidal distance between 1st and 2nd ECEI views $R_* \Delta \phi$ is ~ 87.1 cm. The latter two yields the pitch of the ELM filaments, $\tan \alpha_* = \lambda_{pol} / \lambda_{tor} \approx \Delta y / (R_* \Delta \phi) \approx 0.17$. Using Eq. (3) and measured $R_* = 222$ cm of the ELM filaments, we obtain $n \approx 7.0$. This number is consistent with the mode analysis result of the Mirnov coils (Fig. 5), in which the contour plot of the band-pass filtered Mirnov coil signals clearly shows the mode structure of $n = 7$. The ECEI measurement error due to finite spatial resolution and imperfection in the optical alignment can result in over- or under-estimation of λ_{pol} and $\tan \alpha_*$, which can lead to an error up to ± 1 in n .

Table I contains the measurements of $\tan \alpha_*$ obtained using EFIT and 3D ECEI with the corresponding mode numbers denoted as n_{EFIT} and n_{ECEI} , which are compared with the mode number n_{Mirnov} determined by the analysis of Mirnov coil array signals; 27 of the 28 estimates are identical with

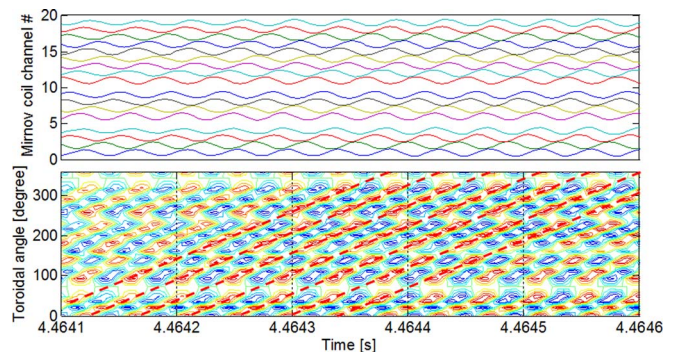


FIG. 5. Contour plot of Mirnov signals for analysis of toroidal mode number n . A few dead channels among the 20 Mirnov coils in the KSTAR device were omitted in this plot. By comparing the number of the same phase at a single arbitrary time, $n = 7$ is obtained.

TABLE I. Comparison of results from ECEI and Mirnov coils. The pitch angle α_* was determined using EFIT and 3D ECEI. Estimations obtained using the two methods are consistent with Mirnov coil measurement. Note that n must be an integer, so the estimates were rounded (\rightarrow) to the nearest integer.

Shot	Time [s]	λ_{pol} [cm]	$\tan \alpha_*$ (EFIT)	n_{EFIT}	$\tan \alpha_*$ (ECEI)	n_{ECEI}	n_{Mirnov}	Error
8114	2.575	58.3	0.169	3.994	0.169	3.974	4	0
8114	2.670	56.4	0.169	4.114	0.169	4.104	4	0
8114	2.694	57.1	0.170	4.104	0.169	4.054	4	0
8114	2.743	54.9	0.168	4.194	0.169	4.224	4	0
8114	2.812	53.7	0.170	4.334	0.169	4.314	4	0
8142	2.905	48.7	0.143	4.034	0.148	4.184	4	0
8142	3.093	46.1	0.142	4.244	0.148	4.404	4	0
8142	3.141	46.3	0.141	4.184	0.148	4.394	4	0
7328	4.225	44.4	0.156	4.865	0.173	5.405	5	0
7328	4.499	45.6	0.157	4.775	0.173	5.255	5	0
7328	4.530	46.2	0.157	4.715	0.173	5.185	5	0
7323	3.375	50.1	0.183	5.055	0.173	4.775	5	0
7323	3.592	51.1	0.188	5.105	0.173	4.685	5	0
8114	2.550	46.4	0.170	5.015	0.173	5.115	5	0
8114	2.600	46.4	0.170	5.025	0.173	5.115	5	0
8114	3.195	45.4	0.167	5.025	0.173	5.225	5	0
7328	4.524	37.9	0.157	5.746	0.169	6.136	6	0
7323	3.382	43.0	0.183	5.886	0.189	6.086	6	0
7323	3.400	43.5	0.183	5.816	0.189	6.016	6	0
7323	3.414	42.9	0.183	5.896	0.189	6.096	6	0
7323	3.715	43.5	0.190	6.026	0.189	6.016	6	0
8114	2.684	39.1	0.171	5.996	0.173	6.076	6	0
8114	2.695	38.7	0.170	6.036	0.173	6.136	6	0
8142	3.516	34.2	0.140	5.636	0.148	5.946	6	0
7328	4.464	34.1	0.172	7.047	0.171	6.997	7	0
8134	2.200	31.1	0.175	7.798	0.173	7.708	7	1
7328	4.365	27.6	0.157	7.868	0.169	8.448	8	0
7328	4.417	28.6	0.155	7.498	0.169	8.148	8	0

those obtained using the Mirnov coil array, demonstrating the accuracy of n_{ECEI} or n_{EFIT} based on our method. Note that the table contains only cases where n_{Mirnov} were available and there are numerous cases where the Mirnov signals were too weak to determine the mode structure. The estimate of $\tan \alpha_*$ obtained using 3D measurement is consistent with the EFIT result; this means that n can be estimated using a 2D ECE image and EFIT without requiring the more difficult 3D ECEI measurement. This approach will be a powerful tool to estimate n because the EFIT provides relatively accurate $\tan \alpha_*$ in the plasma edge region even using only external magnetics.¹⁷

We conclude that the method described here using either 3D ECEI or the combined 2D ECEI and EFIT provides an accurate estimate of n with absolute error ≤ 1 , and is much better than the conventional method using Mirnov coils, which is often unreliable for instabilities with weak perturbation amplitude or large n .

V. SUMMARY

This paper presents a new and accurate method to estimate the toroidal mode number n of ELM filaments in the KSTAR based on the measurement of the poloidal mode spacing and pitch angle of the filaments. This method can extend the measurable range of n beyond the Nyquist limit of the conventional Mirnov coil array and can work in the absence

of usable Mirnov coil signals. It is also found that the pitch angle measurement can be replaced by EFIT, which enables an easier way of toroidal mode number estimation using only one ECEI.

ACKNOWLEDGMENTS

The authors thank the KSTAR team for supporting the experiments. This work was supported by the NRF Korea Grant No. NRF-2009-0082507 and the (U.S.) Department of Energy (DOE) under Contract No. DE-FG02-99ER54531.

¹H. Zohm, "Edge localized modes (ELMs)," *Plasma Phys. Controlled Fusion* **38**(2), 105 (1996).

²J. W. Connor, "Edge-localized modes - physics and theory," *Plasma Phys. Controlled Fusion* **40**(5), 531 (1998).

³K. Kamiya, N. Asakura, J. Boedo, T. Eich, G. Federici, M. Fenstermacher, K. Finken, A. Herrmann, J. Terry, B. Koch *et al.*, "Edge-localized modes: Recent experimental findings and related issues," *Plasma Phys. Controlled Fusion* **49**(7), S43 (2007).

⁴P. B. Snyder, H. R. Wilson, J. R. Ferron, L. L. Lao, A. W. Leonard, T. H. Osborne, A. D. Turnbull, D. Mossessian, M. Murakami, and X. Q. Xu, "Edge localized modes and the pedestal: A model based on coupled peeling-ballooning modes," *Phys. Plasmas* **9**, 2037 (2002).

⁵H. R. Wilson, S. C. Cowley, A. Kirk, and P. B. Snyder, "Magnetohydrodynamic stability of the H-mode transport barrier as a model for edge localized modes: An overview," *Plasma Phys. Controlled Fusion* **48**(5A), A71 (2006).

⁶A. Kirk, H. R. Wilson, G. F. Counsell, R. Akers, E. Arends, S. C. Cowley, J. Dowling, B. Lloyd, M. Price, and M. Walsh, "Spatial and temporal structure of edge-localized modes," *Phys. Rev. Lett.* **92**(24), 245002 (2004).

- ⁷T. Eich, A. Herrmann, J. Neuhauser, R. Dux, J. C. Fuchs, S. Günter, L. D. Horton, A. Kallenbach, P. T. Lang, C. F. Maggi *et al.*, "Type-I ELM substructure on the divertor target plates in ASDEX Upgrade," *Plasma Phys. Controlled Fusion* **47**(6), 815 (2005).
- ⁸G. S. Yun, W. Lee, M. J. Choi, J. Lee, H. K. Park, B. Tobias, C. W. Domier, N. C. Luhmann, Jr., A. J. H. Donné, and J. H. Lee, "Two-dimensional visualization of growth and burst of the edge-localized filaments in KSTAR H-mode plasmas," *Phys. Rev. Lett.* **107**(4), 045004 (2011).
- ⁹G. S. Yun, W. Lee, M. J. Choi, J. B. Kim, H. K. Park, C. W. Domier, B. Tobias, T. Liang, X. Kong, N. C. Luhmann *et al.*, "Development of KSTAR ECE imaging system for measurement of temperature fluctuations and edge density fluctuations," *Rev. Sci. Instrum.* **81**(10), 10D930 (2010).
- ¹⁰H. K. Park, N. C. Luhmann, Jr., A. J. H. Donné, I. G. J. Classen, C. W. Domier, E. Mazzucato, T. Munsat, M. J. van de Pol, and Z. Xia, "Observation of high-field-side crash and heat transfer during sawtooth oscillation in magnetically confined plasmas," *Phys. Rev. Lett.* **96**(19), 195003 (2006).
- ¹¹G. S. Yun, W. Lee, M. J. Choi, J. Lee, H. K. Park, C. W. Domier, N. C. Luhmann, Jr., B. Tobias, A. J. H. Donné, J. H. Lee *et al.*, "Two-dimensional imaging of edge-localized modes in KSTAR plasmas unperturbed and perturbed by $n = 1$ external magnetic fields," *Phys. Plasmas* **19**, 056114 (2012).
- ¹²I. G. J. Classen, E. Westerhof, C. W. Domier, A. J. H. Donné, R. J. E. Jaspers, N. C. Luhmann, Jr., H. K. Park, M. J. van de Pol, G. W. Spakman, and M. W. Jakubowski, "Effect of heating on the suppression of tearing modes in tokamaks," *Phys. Rev. Lett.* **98**(3), 035001 (2007).
- ¹³B. J. Tobias, I. G. J. Classen, C. W. Domier, W. W. Heidbrink, N. C. Luhmann, Jr., R. Nazikian, H. K. Park, D. A. Spong, and M. A. Van Zeeland, "Fast ion induced shearing of 2D Alfvén eigenmodes measured by electron cyclotron emission imaging," *Phys. Rev. Lett.* **106**(7), 075003 (2011).
- ¹⁴T. Kass, S. Günter, M. Maraschek, W. Suttrop, and H. Zohm, "Characteristics of type I and type III ELM precursors in ASDEX Upgrade," *Nucl. Fusion* **38**(1), 111 (1998).
- ¹⁵H. Reimerdes, A. Pochelon, and W. Suttrop, "Toroidally asymmetric ELM precursors in TCV," *Nucl. Fusion* **38**(3), 319 (1998).
- ¹⁶L. L. Lao, H. St. John, R. D. Stambaugh, A. G. Kellman, and W. Pfeiffer, "Reconstruction of current profile parameters and plasma shapes in tokamaks," *Nucl. Fusion* **25**(11), 1611 (1985).
- ¹⁷Y. S. Park, S. A. Sabbagh, J. M. Bialek, J. W. Berkery, S. G. Lee, W. H. Ko, J. G. Bak, Y. M. Jeon, J. K. Park, J. Kim *et al.*, "Investigation of MHD instabilities and control in KSTAR preparing for high beta operation," *Nucl. Fusion* **53**(8), 083029 (2013).